ISSN 2347-3487

Mixed convection flow due to a moving vertical plate parallel to free stream under the influence of Newtonian heating and thermal radiation

P. M. Patil*[a] and S. Roy[b]
[a]Department of Mathematics, Karnatak University, Pavate nagar, Dharwad – 580 003, India.
[b]Department of Mathematics, IIT Madras, Chennai-600036, India.
E-mail address: pmpatil@kud.ac.in (P. M. Patil) and sjroy@iitm.ac.in (S. Roy)

ABSTRACT

The steady mixed convection flow from a moving vertical plate in a parallel free stream is considered to investigate the combined effects of buoyancy force and thermal diffusion in presence of thermal radiation as well as Newtonian heating effects. The governing boundary layer equations are transformed into a non-dimensional form by a group of non-similar transformations. The resulting system of coupled non-linear partial differential equations is solved by an implicit finite difference scheme in conjunction with the quasi-linearization technique. Computations are performed and representative set is displayed graphically to illustrate the influence of the mixed convection parameter (λ), Prandtl number (*Pr*), the ratio of free stream velocity to the composite reference velocity (ε) and the radiation parameter (*R*) on the velocity and temperature profiles. The numerical results for the local skinfriction coefficient ($\mathrm{Re}_L^{1/2} C_f$) and surface temperature ($G_W(\xi,0)$) are also presented. The results show that the streamwise co-ordinate ξ significantly influences the flow and thermal fields which indicate the importance of non-similar solutions. Also, it is observed that the increase of mixed convection parameter (λ) causes the increase in the magnitude of velocity profile about 65% for lower Prandtl number fluids (*Pr*=0.7), while it decreases in the temperature profile about 30%. Present results are compared with previously published work and are found to be in excellent agreement.

KEYWORDS

Mixed convection; moving plate; parallel free stream; thermal radiation; Newtonian heating.

ISSN 2347-3487

1. Introduction

The phenomenon of boundary layer behavior over a moving plate in a parallel free stream has more important practical applications such as the aerodynamic extrusion of plastic sheets, the cooling of an infinite metallic plate in a cooling bath, the boundary layer along material handling conveyers, the boundary layer along a liquid film in condensation processes, paper production etc. Tsou *et al*. [1] have showed experimentally that the flow and heat transfer problem from a continuously moving surface is a physically realizable one and studied its basic characteristics. Chappidi and Gunnerson [2] have studied the laminar boundary layer in two cases $U_w > U_\infty$ and $U_\infty > U_w$ separately and formulated two sets of boundary value problems. Afzal *et al*. [3] formulated a single set of boundary conditions by employing the composite reference velocity $U = U_w + U_\infty$, where U_w is the moving plate velocity and U_∞ is the free stream velocity, instead of considering U_w and U_∞ separately, irrespective of whether $U_w > U_\infty$ or $U_\infty > U_w$. Lin and Haung [4] were analyzed for horizontal isothermal plate moving in parallel or reversibly to a free stream where similarity and non-similarity equations are used to obtain the flow and thermal fields. Sparrow and Abraham [5] used the relative velocity model where only one of the participating media is in motion. Karwe and Jaluria [6] presented numerical simulation of thermal transport associated with a continuously moving flat sheet in material processing. The steady laminar flow and heat transfer characteristics of a continuously moving vertical sheet of extruded material are studied close to and far downstream from the extrusion slot by Al-sanea [7]. Soundalgekar and Murty [8] have discussed the effects of power law surface temperature variation on the heat transfer from a continuous moving surface with constant surface velocity. More recently, Cortell [9] extended the work of Afzal *et al.* [3] by taking viscous dissipation effect in the energy balance. The effects of transpiration on the flow and heat transfer over a moving permeable surface in a parallel stream are analyzed by Ishak *et al.* [10]. The development of the boundary layer on a fixed or moving surface parallel to a uniform free stream in presence of surface heat flux has been investigated by Ishak *et al.* [11]. Patil *et al*. [12] have examined the role of internal heat generation or absorption effects on the flow and heat transfer over a moving vertical plate. In this study, authors have considered the steady flow and heat transfer characteristics.

The comprehensive analysis on steady mixed convection flow due to a moving semi-infinite vertical plate in a parallel free stream with thermal diffusion is also important to be investigated and such studies are yet to appear in the literature. Furthermore, steady mixed convection flows do not necessarily posses similarity solutions in many flow patterns. The nonsimilarity in such flows may be due to the free stream velocity or due to the curvature of the body or due to the surface mass transfer or even possibly due to all these effects. A solution is called self-similar if a system of partial differential equations can be reduced to a system of ordinary differential equations. If the similarity transformations are only able to reduce the number of independent variables, then the transformed equations are called as semi-similar and the corresponding solutions are the semi-similar solutions. Therefore, as a step towards the eventual development of studies on steady mixed convection flows it is important as well as useful to investigate the combined effects of buoyancy and thermal diffusion on a steady mixed convection flow along a semi-infinite vertical plate.

The objective of this study is to analyze the simultaneous effects of buoyancy and thermal diffusion on a mixed convection flow from a semi-infinite vertical plate in presence of thermal radiation and Newtonian heating effects. The plate is supposed to move parallel to the free stream velocity. The coupled non-linear partial differential equations governing the flow have been solved numerically using an implicit finite difference scheme in combination with the quasi-linearization technique [13-17]. The results are revealing that interesting features of flow and heat transfer phenomena.

2. Mathematical formulation

We **c**onsider the steady laminar viscous and incompressible mixed convection boundary layer flow along a semi-infinite vertical plate moving with velocity U_W in the x- direction subjected to Newtonian heating effects. The x-axis is taken along the plate in the vertically upward direction and the y- axis is taken normal to it. A schematic representation of the physical model and co-ordinates system is depicted in Fig. 1. The buoyancy force arises due to the temperature difference in the fluid. The fluid is considered to be gray; absorbing-emitting radiation but non-scattering medium and the Rosseland approximation [18] is used to describe the radiative heat flux in the x- direction is considered negligible in comparison to the y- direction. All thermo-physical properties of the fluid in the flow model are assumed constant except the density variations causing a body force in the momentum equation. The Boussinesq approximation is invoked for the fluid properties to relate density changes, and to couple in this way the temperature field to the flow field (Schlichting and Gersten [19]). Under these assumptions, the dimensional equations of conservation of mass, momentum and energy governing the steady mixed convection boundary layer flow over a moving vertical plate are given by

$$\frac{\partial u}{\partial x} + \frac{\partial v}{\partial y} = 0, \tag{1}$$

$$u\frac{\partial u}{\partial x} + v\frac{\partial u}{\partial y} = \nu\frac{\partial^2 u}{\partial y^2} + g\,\beta\left(T - T_\infty\right), \tag{2}$$

$$u\frac{\partial T}{\partial x}+v\frac{\partial T}{\partial y}=\left(\frac{k}{\rho C_p}\right)\frac{\partial^2 T}{\partial y^2}-\left(\frac{1}{\rho C_p}\right)\frac{\partial q_r}{\partial y}, \tag{3}$$

where all the physical quantities is mentioned in the Nomenclature.

The physical boundary conditions are given by

$$\begin{aligned} &y=0: u=U_w, \quad v=0, \quad \frac{\partial T}{\partial y}=-h_s T, \\ &y\to\infty: u\to U_\infty, \qquad T\to T_\infty. \end{aligned} \tag{4}$$

The radiation heat flux q_r under Rosseland approximation Brewster [18], we take

$$q_r=-\frac{4\sigma_{SB}}{3a_R}\frac{\partial T^4}{\partial y} \tag{5}$$

where σ_{SB} is the Stefan-Boltzmann constant and a_R is the Rosseland mean spectral absorption coefficient.

We assume that the temperature difference within the flow are sufficiently small such that T^4 can be expressed as a linear function of temperature. We now expand T^4 in a Taylor series about T_∞ as follows:

$$T^4=T_\infty^{\,4}+4T_\infty^{\,3}\left(T-T_\infty\right)+6T_\infty^{\,2}\left(T-T_\infty\right)^2+---------- \tag{6}$$

Neglecting higher order terms in the above equation beyond the first degree in (T - T_∞), we get,

$$T^4\cong -3T_\infty^{\,4}+4T_\infty^{\,3}T \tag{7}$$

In view of Eqs. (5) and (7), the Eq. (3) becomes

$$u\frac{\partial T}{\partial x}+v\frac{\partial T}{\partial y}=\alpha\left(1+\frac{16\sigma_{SB}T_\infty^3}{3k\,a_R}\right)\frac{\partial^2 T}{\partial y^2} \tag{8}$$

where $\alpha=k/(\rho C_p)$ is the thermal diffusivity.

We now introducing the following transformations:

$$\xi=\frac{x}{L};\ \eta=\left(\frac{U}{\nu x}\right)^{1/2}y;\quad \psi(x,y)=(\nu U x)^{1/2}\,f(\xi,\eta);$$

$$u=U\,f_\eta=U\,F;\ U=U_\infty+U_w;\ v=-\frac{(\nu x U)^{1/2}}{2x}\left\{f(\xi,\eta)+2\xi f_\xi-\eta f_\eta\right\};$$

$$T-T_\infty=T_\infty G(\xi,\eta); \tag{9}$$

where ψ is the stream function, which is defined as $u=\partial\psi/\partial y$ and $v=-\partial\psi/\partial x$. Substituting transformations (9) into Eqs. (1) - (2) and (8), we find that Eq. (1) is identically satisfied and Eqs. (2) and (8) reduce to

$$F_{\eta\eta}+\frac{f}{2}F_\eta+\lambda\xi G=\xi\left(F F_\xi-f_\xi F_\eta\right), \tag{10}$$

$$\left(\frac{1+R}{\mathrm{Pr}}\right)G_{\eta\eta}+\frac{f}{2}G_\eta=\xi\left(F G_\xi-f_\xi G_\eta\right). \tag{11}$$

The corresponding non-dimensional Boundary conditions:

$$F = 1-\varepsilon, \quad G_\eta = -\xi^{1/2}(1+G), \quad \text{at} \quad \eta = 0,$$
$$F \to \varepsilon, \qquad G \to 0, \quad \text{as} \quad \eta \to \infty. \tag{12}$$

Here $f = \int_0^\eta F\, d\eta$, $\Pr = \nu/\alpha$ is the Prandtl number, $R = 16\sigma_{SB} T_\infty^3/(3k\, a_R)$ is the radiation parameter and we take $h_s = \mathrm{Re}_L^{1/2}/L$ (see Merkin [20]). Further, λ is the mixed convection parameter and ε is the ratio of free stream velocity to the composite reference velocity parameter, which are defined as

$$\lambda = \frac{Gr}{\mathrm{Re}_L^2}, \quad \varepsilon = \frac{U_\infty(x)}{U(x)} = \frac{U_{\infty 0}}{U_{\infty 0} + U_{w0}}, \tag{13}$$

where $Gr = g\,\beta T_\infty L^3/\nu^2$ is the Grashof number referring to the wall temperature and $\mathrm{Re}_L = U\,L/\nu$ is the local Reynolds number. It should be mentioned that $\lambda > 0$ ($T_w(x) > T_\infty$) corresponds to the assisting flow, $\lambda < 0$ ($T_w(x) < T_\infty$) corresponds to opposing flow and $\lambda = 0$ ($T_w(x) = T_\infty$) corresponds to the forced convection flow case. We also notice that $\varepsilon = 1$ corresponds to a fixed (static) plate, while $\varepsilon = 0$ corresponds to a moving plate, respectively. It may be remarked that a single constant, "*Pr*/(1+*R*)" known as "$Pr_{\text{effective}}$" [21], can display the effects of radiation (*R*) and Prandtl number (*Pr*) when the sole interest is to study the effects of radiation (*R*) and Prandtl number (*Pr*) for a wide range of parameter values. In such situation a single parameter "*Pr*/(1+*R*)" known as "$Pr_{\text{effective}}$" [21] could serve the purpose for the whole range of parameter values. Since the present study concerned about the effect of Newtonian heating only for air (*Pr* = 0.7) and water (*Pr* = 7.0), numerical results are presented by indicating known *Pr* values of air (*Pr* = 0.7) and water (*Pr* = 7.0).

The main physical quantities of interest are the skin friction coefficient $\mathrm{Re}_L^{1/2} C_f$ and the wall temperature $G_W(\xi, 0)$. These quantities are defined respectively, as

$$\mathrm{Re}_L^{1/2} C_f = \xi^{-1/2} F_\eta(\xi, 0), \quad G_w(\xi, 0) = -\left[1 + \xi^{-1/2} G_\eta(\xi, 0)\right]. \tag{14}$$

3. Method of solution

The set of coupled non-linear partial differential Equations (10) – (11) under the boundary conditions (12), represent a non-linear two point boundary value problem for partial differential equations which is solved numerically using an implicit finite difference scheme in combination with the quasi-linearization technique [13-17]. An iterative sequence of linear equations is carefully constructed to approximate the non-linear Eqs. (10) – (11) under the boundary conditions (12) achieving quadratic convergence and monotonicity of the sequence of solutions.

Applying the quasi-linearization technique [13-17], the non-linear coupled partial differential equations (10) - (11) are replaced by the following sequence of linear partial differential equations:

$$F_{\eta\eta}^{(i+1)} + A_1^i F_\eta^{(i+1)} + A_2^i F^{(i+1)} + A_3^i F_\xi^{(i+1)} + A_4^i G^{(i+1)} = A_5^i \tag{15}$$

$$G_{\eta\eta}^{(i+1)} + B_1^i G_\eta^{(i+1)} + B_2^i G_\xi^{(i+1)} + B_3^i F^{(i+1)} = B_4^i \tag{16}$$

The coefficient functions with iterative index *i* are known and the functions with iterative index (*i*+1) are to be determined. The corresponding boundary conditions are given by:

$$F^{i+11} = 1-\varepsilon, \quad G_\eta^{i+1} = -\xi^{1/2}(1+G^{i+1}), \quad \text{at} \quad \eta = 0,$$
$$F^{i+1} \to \varepsilon, \quad G^{i+1} \to 0, \quad \text{as} \quad \eta \to \eta_\infty. \tag{17}$$

The resulting sequence of linear partial differential equations (15) and (16) were discretisized using second order central difference formula in η - direction and backward difference formula in ξ - direction. In each iteration step, the equations were then reduced to a system of linear algebraic equations, with a block tri-diagonal structure which is solved using Varga's algorithm [22]. To ensure the convergence of the numerical solution to the exact solution, step sizes $\Delta\eta$ and $\Delta\xi$ are optimized and the results presented here are independent of the step sizes at least up to the fourth decimal place. A convergence criterion based on the relative difference between the current and previous iteration values is employed. The solution is assumed to have converged and the iteration process is terminated when the difference reaches i.e.

$$\text{Max}\left\{\left|\left(F_\eta\right)_w^{\,i+1}-\left(F_\eta\right)_w^{\,i}\right|,\ \left|\left(G_\eta\right)_w^{\,i+1}-\left(G_\eta\right)_w^{\,i}\right|\right\}<10^{-4}. \quad (18)$$

4. Results and discussion

The comprehensive numerical parametric study was conducted and results are reported in terms of graphs. This is done to illustrate special features of solutions. The computations have been carried out for various values of $\Pr\left(0.7\le\Pr\le 7.0\right)$, $\lambda\left(-0.25\le\lambda\le 5.0\right)$, $\varepsilon\left(0.1\le\varepsilon\le 0.9\right)$, $R\left(0.0\le R\le 1.0\right)$, and $\xi\left(0\le\xi\le 1\right)$. The edge of the boundary layer $\left(\eta_\infty\right)$ has been taken between 8.0 and 18.0 depending on the values of the parameters. Afzal *et al*. [3] have discussed only self-similar solutions where all solutions along streamwise direction were made congruent using similarity transformations. Governing equations were finally reduced to a set of ordinary differential equations. In such cases, single asymptotic solution will not be able to represent all physical solutions. Further, it is reported by many other investigators also that there are dual solutions with different asymptotic nature. In contrast, authors have captured non-similar solutions at each streamwise location by solving coupled set of partial differential equations. In this investigation, authors have observed a single non-similar solution at each streamwise location. It may be noted that ξ = 0 is a singular point while obtaining the non-similar solutions and results are valid only for ξ > 0. Further, ξ = 0 results are obtained separately and compared with the existing results in literature as displayed in Table 1. Also, results show an excellent agreement with the results reported by earlier investigators.

In order to verify the correctness of the present investigation, steady state results of heat transfer rate $\left[-G_\eta\left(0\right)\right]$ are compared with the results previously reported by Tsou *et al*. [1], Soundalgekar and Murty [8], and Patil *et al.* [12]. Some of the comparisons are presented in Table 1 and are found to be in excellent agreement.

The effects of Prandtl number (*Pr*) and buoyancy (mixed convection) parameter $\left(\lambda\right)$ on velocity and temperature profiles $\left(F\left(\xi,\eta\right),G\left(\xi,\eta\right)\right)$ as well as skin friction coefficient and wall temperature $\left(\text{Re}_L^{\,1/2}C_f,G_W\left(\xi,0\right)\right)$ when ε = 0.5, *R* = 0.5 and $\xi=1$ are displayed in Figs. 2 - 5. The influence of buoyancy assisting force $\left(\lambda>0\right)$ shows the significant overshoot in the velocity profiles $F\left(\xi,\eta\right)$ near the plate for lower Prandtl number (*Pr*) fluids (air, *Pr* = 0.7) while for higher Prandtl number (*Pr*) fluids (water, *Pr* = 7.0), the velocity overshoot is not observed as shown in Fig. 2. The magnitudes of the velocity overshoot increases with the buoyancy parameter $\left(\lambda>0\right)$ while it decreases as Prandtl number (*Pr*) increases. The physical reason is that the buoyancy force $\left(\lambda\right)$ effect is more in lower Prandtl number (*Pr*) fluid (air, *Pr* = 0.7) due to the lower viscosity of the fluid enhances the velocity profile within the stretching boundary layer as the assisting buoyancy force $\left(\lambda\right)$ acts like a favourable pressure gradient and hence, the velocity overshoot occurs. For higher Prandtl number (*Pr*) fluids (water, *Pr* = 7.0), the overshoot is not present because higher Prandtl number (*Pr*) fluids implies more viscous fluid which have less impact on the buoyancy parameter $\left(\lambda\right)$. For example, ε = 0.5, *R* = 1.0 and *Pr* = 0.7 when $\lambda=5$, the velocity profile $F\left(\xi,\eta\right)$ is enhanced approximately by 65% for lower Prandtl number fluids as compared to the higher Prandtl number fluids. The effect of buoyancy opposing force on velocity and temperature profiles is also presented in Figs. 2 and 3 by a representative negative value of λ $\left(\lambda=-0.25\right)$ to limit the number of lines in the figures. It is worthy to note from the Fig. 2 that for opposing buoyancy flow (λ < 0), the buoyancy opposing force reduces the magnitude of the velocity significantly within the moving boundary layer for low Prandtl number fluid (*Pr* = 0.7, air) as well as for high Prandtl number fluid (*Pr* = 7.0, water). The influence of buoyancy parameter $\left(\lambda\right)$ has relatively less influence on the temperature profiles $G\left(\xi,\eta\right)$, as shown in Fig. 3. Furthermore, Fig. 3 also show that the effect of higher Prandtl number fluids (water, *Pr* = 7.0) results into a thinner thermal boundary layer since the higher Prandtl number (*Pr*) fluids (water, *Pr* = 7.0) have lower thermal conductivity. Figures 4 and 5 represent the influence of mixed convection parameter λ and Prandtl number on the skin friction coefficient and wall temperature $\left(\text{Re}_L^{\,1/2}C_f,G_W\left(\xi,0\right)\right)$. Skin friction coefficient increases with the increase of buoyancy parameter $\left(\lambda\right)$ while wall temperature $G_W\left(\xi,0\right)$ decreases. The physical reason is that the buoyancy force $\left(\lambda>0\right)$ implies favorable pressure gradient, and the fluid gets accelerated, which results in thinner momentum and

thermal boundary layers. Further, when Prandtl number *Pr* increases from 0.7 to 7.0, the wall temperature $G_W(\xi,0)$ as well as skin friction coefficient $\left(\mathrm{Re}_L^{1/2} C_f\right)$ decrease, as shown in Figs. 4 and 5. For example, when ε = 0.5, *R* = 0.5 and $\xi=1$, $\left(\mathrm{Re}_L^{1/2} C_f\right)$ increases approximately about 281% and 299% as λ increases from 1.0 to 5.0 for *Pr* = 0.7 and for *Pr* = 7.0 (see Fig.4), respectively. Furthermore, Figure 5 shows that wall temperature $G_W(\xi,0)$ decreases approximately about 5% and 11%, respectively, for *Pr* = 0.7 and for *Pr* = 7.0 when λ increases from 1.0 to 5.0.

Figure 6 displays the effect of ε (the ratio of free stream velocity to the composite reference velocity) and the thermal radiation parameter *R* on the velocity profile $F(\xi,\eta)$ with λ = 1.0, ξ = 1 and *Pr* = 0.7. The velocity is strongly depending on ε because it occurs in the governing momentum equation as well as in the boundary condition for the velocity profile $F(\xi,\eta)$. It has been observed that the magnitude of the velocity profile within the moving boundary layer increases with the increase of ε, while it decreases as *R* increases from R = 0.0 to R = 1.0. The physical reason is that the assisting buoyancy force due to thermal gradients as well as increase in ε act likes a combined favorable pressure gradient which accelerates the fluid for uniform motion. The effect of radiation is to decrease the rate of energy transport to the fluid, thereby decreasing the temperature and velocity of the fluid.

Figure 7 illustrates the role of stream wise coordinate ξ and thermal radiation parameter *R* on the temperature profile $G(\xi,\eta)$ when ε = 0.5, $\lambda=1.0$ and *Pr* = 0.7. The temperature profile $G(\xi,\eta)$ is decreasing with stream wise co-ordinate ξ as it increases from 0 to 1. Also, the temperature profile $G(\xi,\eta)$ is to decrease with thermal radiation parameter for both at $\xi=0$ and $\xi=1$. This clearly indicates that an increase in stream wise coordinate ξ acts as a decelerating pressure gradient and thus fluid flows slower. As a result, $G(\xi,\eta)$ decreases. In particular, for example; ε = 0.5, $\lambda=1.0$, *R* = 0.2 and *Pr* = 0.7 at $\eta=6.0$, the temperature profile $G(\xi,\eta)$ is reduced approximately by 46% as ξ increases from 0.0 to 1.0.

5. Conclusions

A numerical study is performed for the problem of steady mixed convection flow over a moving vertical plate in a parallel free stream in the presence of Newtonian heating applied at the wall and the thermal radiation. We draw the following conclusions in the investigation:

- Mixed convection parameter λ enhances the skin friction coefficient while the surface temperature is reduced.
- From the computed results, it is found that in presence of buoyancy force $(\lambda>0)$, the velocity profile exhibits velocity overshoot 65% more for lower Prandtl number (*Pr* = 0.7) as compared to the magnitude of the velocity overshoot for higher Prandtl number (*Pr* = 7.0) fluid.
- The effect of thermal radiation leads to a fall in the momentum and thermal boundary layers. Further, it is noted that the thermal radiation parameter to increase the surface temperature.
- The magnitude of the velocity profile within the moving boundary layer increases about 45% with the increase of ε (the ratio of free stream velocity to the composite reference velocity) from 0.1 to 0.9, while it decreases about 30% as *R* increases from R = 0.0 to R = 1.0.
- The temperature profile $G(\xi,\eta)$ decreases with stream wise co-ordinate ξ when it increases from 0 to 1.

Acknowledgement: The author Dr. P. M. Patil has dedicated this paper respectfully to **Prof. H. B. Walikar,** Honourable Vice-Chancellor, Karnatak University, Dharwad – 580 003, India, on the occasion of his Sixty Third birthday.

References

[1] F.K. Tsou, E.M. Sparrow, R.J. Goldstein, (1967) Flow and heat transfer in the boundary layer on a continuous moving surface, Int. J. Heat Mass Transfer **10** (1967) 219-235.

[2] P. R. Chappidi, F. S. Gunnerson, Analysis of heat and momentum transport along a moving surface, Int. J. Heat Mass Transfer **32** (1989) 1383- 1386.

[3]. N. Afzal, A. Baderuddin, A. A. Elgarvi, Momentum and heat transport on a continuous flat surface moving in a parallel stream, Int. J. Heat Mass Transfer **36** (1993) 3399- 3403.

[4]. H. T. Lin, S. F. Haung, Flow and heat transfer of plane surface moving in parallel and reversely to the free stream, Int. J. Heat Mass Transfer **37** (1994) 333- 336.

[5] E. M. Sparrow, J. P. Abraham, Universal solutions for the stream wise variation of the temperature of a moving sheet in the presence of a moving fluid, Int. J. Heat and Mass Transfer, **48** (2005) 3047 – 3056.

[6] M. V. Karwe, Y. Jaluria, Numerical simulation of thermal transport associated with a continuously moving flat sheet in material processing, ASME J. Heat Transfer **113** (1991) 612- 619.

[7] Sami A. Al- Sanea, Mixed convection heat transfer along a continuously moving heated vertical plate with suction or injection, Int. J. Heat Mass Transfer **47** (2004) 1445- 1465.

[8] V.M. Soundalgekar, T.V.R. Murty, Heat transfer in flow past a continuous moving plate with variable temperature, Warme-und Stoffubertragung **14** (1980) 91-93.

[9] R. Cortell, Flow and heat transfer in moving fluid over a moving flat surface, Theoretical Computational Fluid Dynamics. **21** (2007) 435 – 446.

[10] A. Ishak, R. Nazar, I Pop, The effects of transpiration on the flow and heat transfer over a moving permeable surface in a parallel stream, Chemical Engineering Journal, **148** (2008) 63 - 67.

[11] A. Ishak, R. Nazar, I Pop, Flow and heat transfer characteristics in a moving flat plate in a parallel stream with constant surface heat flux, Heat Mass Transfer, **45** (2009) 563 – 567.

[12] P. M. Patil, S. Roy and I. Pop, Flow and heat transfer over moving vertical plate in a parallel free stream; Role of internal heat generation or absorption, Chemical Engineering Communications **199** (5) (2012) 658 - 672.

[13] P. M. Patil, S. Roy, Unsteady mixed convection flow from a moving vertical plate in a parallel free stream: Influence of heat generation or absorption, Int. J. Heat Mass Transfer **53** (2010) 4749 – 4756.

[14] P. M. Patil, S. Roy and Ali J. Chamkha**,** Double diffusive mixed convection flow over a moving vertical plate in presence of internal heat generation and chemical reaction, Turkish Journal of Engineering & Environmental Sciences **33**(3) (2009) 193 – 205.

[15] P. M. Patil, S. Roy and Ali J. Chamkha**,** Mixed convection flow over a vertical power-law stretching sheet, International Journal of Numerical Methods for Heat and Fluid Flow, **20** (4) (2010) 445 – 458.

[16] P. M. Patil, Ali J. Chamkha and S. Roy, Effects of chemical reaction on mixed convection flow of a polar fluid through a porous medium in presence of internal heat generation, Meccanica, **47** (2012) 483 – 499.

[17] P. M. Patil, Effects of surface mass transfer on steady mixed convection flow from vertical stretching sheet with variable wall temperature and concentration, International Journal of Numerical Methods for Heat and Fluid Flow, **22** (3) (2012) 287 – 305.

[18] R. Siegel, J. R. Howell, Thermal Radiation Heat Transfer, 4th Ed., Taylor & Francis, New York (2002).

[19] H. Schlichting and K. Gersten, Boundary Layer Theory, Springer, New York, 2000.

[20] J. H. Merkin, Natural convection boundary layer flow on a vertical surface with Newtonian heating, Int. J. Heat Fluid Flow, **15** (1994) 392 – 398.

[21] E. Magyari, A. Pantokratoras, Note on the effect of thermal radiation in the linearised Rosseland approximation on the heat transfer characteristics of various boundary layer flows, International Communications in Heat and Mass Transfer **38** (2011) 554 – 556.

[22] R. S. Varga, Matrix Iterative Analysis, Prentice Hall, (2000).

ISSN 2347-3487

Nomenclature

C_f	local skin-friction coefficient
C_p	specific heat at constant pressure $\left(J\,K^{-1}\,kg^{-1}\right)$
f	dimensionless stream function
F	dimensionless velocity
g	acceleration due to gravity $\left(m\,s^{-2}\right)$
G	dimensionless temperature
Gr	local Grashof number due to temperature
L	characteristic length $\left(m\right)$
R	radiation parameter
Nu_x	local Nusselt number
Pr	Prandtl number $\left(\nu/\alpha\right)$
Re_L	local Reynolds number
T	temperature $\left(K\right)$
T_∞	ambient temperature $\left(K\right)$
u	velocity component in the x direction $\left(m\,s^{-1}\right)$
v	velocity component in the y direction $\left(m\,s^{-1}\right)$
x, y	Cartesian coordinates $\left(m\right)$

Greek symbols

α	thermal diffusivity $\left(m^2\,s^{-1}\right)$
β	volumetric coefficients of the thermal expansion $\left(K^{-1}\right)$
ξ, η	transformed variables
λ	mixed convection parameter
μ	dynamic viscosity $\left(kg\,m^{-1}\,s^{-1}\right)$
ν	kinematic viscosity $\left(m^2\,s^{-1}\right)$
ρ	density $\left(kg\,m^{-3}\right)$
ψ	streamfunction $\left(m^2\,s^{-1}\right)$

Subscripts

w, ∞	conditions at the wall and infinity, respectively
ξ, η	denote the partial derivatives with respect to these variables, respectively

ISSN 2347-3487

Table 1. Comparison of $-G_\eta(0)$ for $\lambda = 0$, $\xi = 0$, R = 0, $\varepsilon = 0$ and selected values of *Pr*, the plate being isothermal (T_w = constant) to previously published work.

Pr	0.7	1.0	2.0	7.0	10.0	100.0
Tsou *et al*. [1]	0.3492	0.4438	--	--	1.6804	5.545
Soundalgekar and Murty [8]	0.3508	--	0.6831	--	1.6808	--
Patil *et al*. [12]	0.35004	0.44401	0.68314	1.38625	1.68011	5.54610
Present work	0.35005	0.44403	0.68316	1.38627	1.68013	5.54612

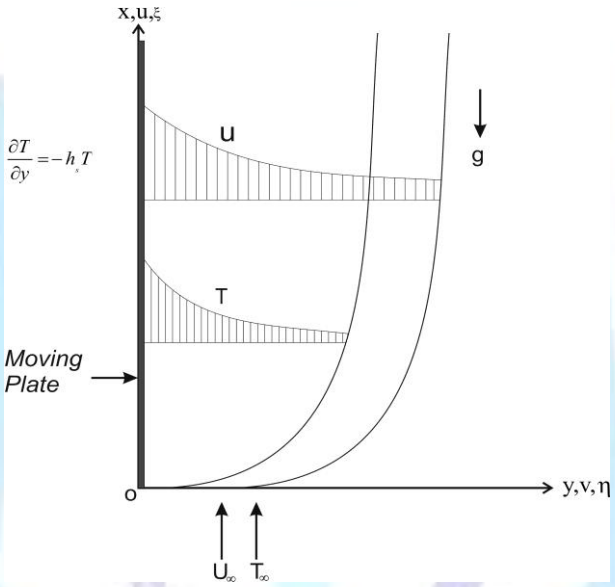

Fig. 1. Schematic diagram and co-ordinates system

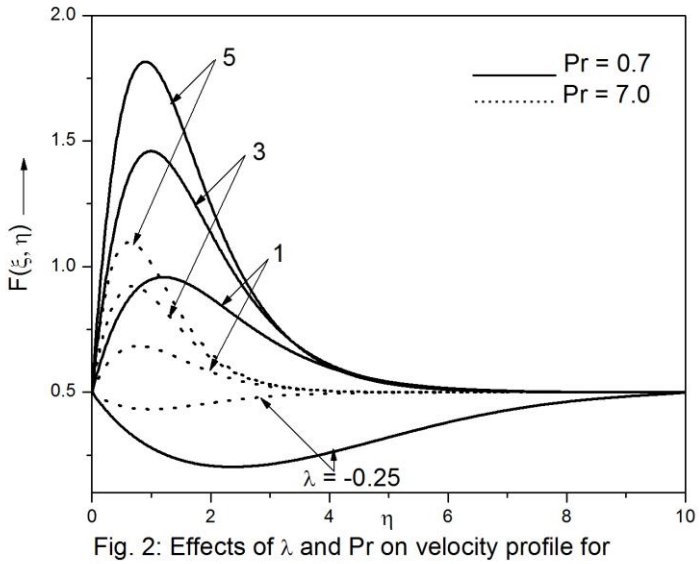

Fig. 2: Effects of λ and Pr on velocity profile for R = 1, ξ = 1 and ε = 0.5.

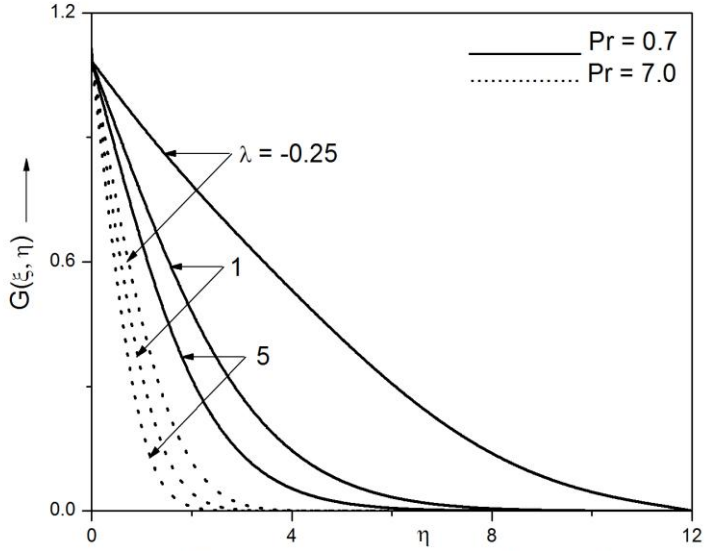

Fig. 3: Effects of λ and Pr on temperature profile for R = 1, ξ = 1 and ε = 0.5.

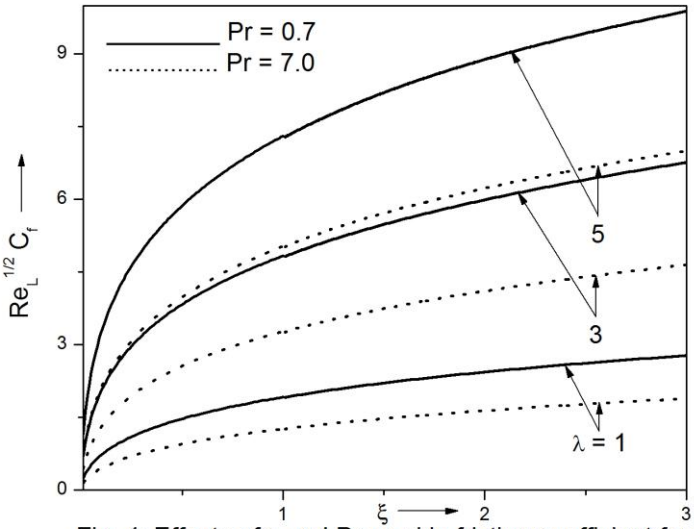

Fig. 4: Effects of λ and Pr on skin friction coefficient for R = 0.5 and ε = 0.5.

ISSN 2347-3487

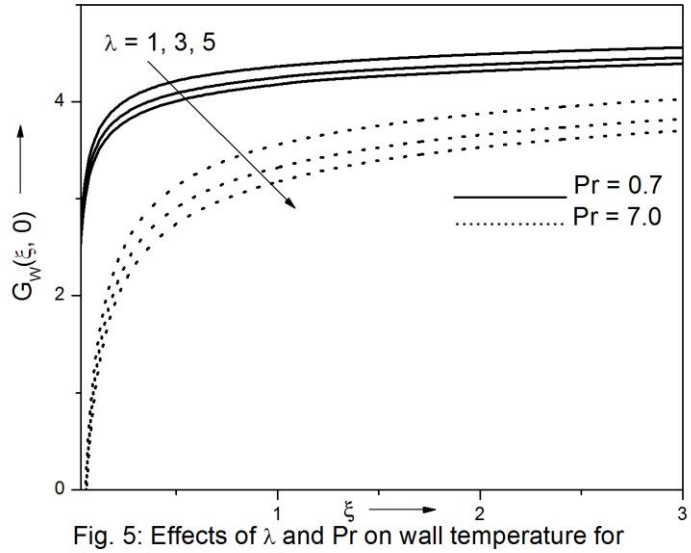

Fig. 5: Effects of λ and Pr on wall temperature for R = 0.5 and ε = 0.5.

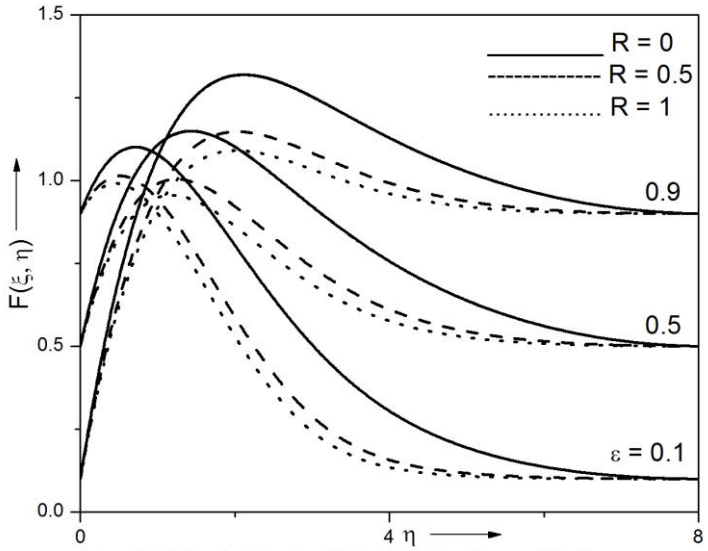

Fig. 6: Effects of ε and R on velocity profile for Pr = 0.7, ξ = 1 and λ = 1.

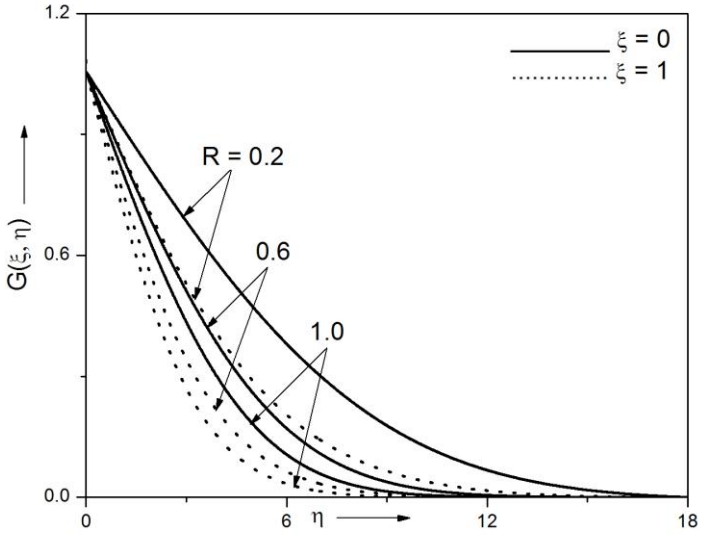

Fig. 7: Effects of ξ and R on temperature profile for Pr = 0.7, ε = 0.5 and λ = 1.